

## Improving dielectric properties of poly(vinylidene fluoride) composites: effects of surface functionalization of exfoliated graphene

Shuaijie Wang, Liangsen Liu, Yan Zeng, Baoming Zhou\*, Kunyue Teng, Meijun Ma, Lei Chen and Zhiwei Xu

*Key Laboratory of Advanced Braided Composites, Ministry of Education, School of Textiles, Tianjin Polytechnic University, Tianjin 300387, P.R. China*

*(Received 24 November 2014; final version received 24 December 2014; accepted 27 December 2014)*

To investigate the effects of surface functionalization of exfoliated graphene (EG) on the crystalline form of  $\beta$ -phase and dielectric properties of poly(vinylidene fluoride) (PVDF), we prepared PVDF-based composites reinforced by different functionalized EG. The X-ray photoelectron spectroscopy results indicated that a wide variety of chemical functional groups such as C–OH, C–O–C, C=O, COOH and C–F could be introduced on the surface of modified EG. As confirmed by results of Fourier transform infrared spectrum and X-ray diffraction, the  $\beta$ -phase PVDF can be produced in the composites with the incorporation of functionalized EG. In the frequency ranging from  $10^2$  to  $10^7$  Hz, the dielectric permittivity of PVDF composites shows an obvious increase owing to a variation of the carbonyl group (C=O) content. Among all the composites, the EG grafted with polymethyl methacrylate/PVDF composite has the highest dielectric permittivity and dielectric loss.

**Keywords:** functionalized graphene;  $\beta$ -phase; dielectric permittivity; carbonyl group

### 1. Introduction

Polymer-based composites with excellent dielectric performance are currently very popular topics in the field of materials science and have received increasing attention in recent years.[1] Compared with the traditional ceramic ferroelectric materials, poly(vinylidene fluoride) (PVDF) has good electrical properties, high mechanical strength, good flexibility, and good chemical stability and can be easily prepared in low temperature.[2,3] Due to piezoelectricity and pyroelectricity in the crystalline form of  $\beta$ -phase, PVDF is widely used in transducers, piezoelectric sensor, infrared imaging, and other military and biomedical fields,[4–6] and its excellent dielectric and ferroelectric performance in contrast to other polymers endows promising applications in energy storage materials.[7,8] However, PVDF has low dielectric permittivity. Therefore, the new methods for improving the dielectric permittivity of PVDF have been explored always.

It is reported that a small volume fraction of some conductive filler was added to the polymer matrix to achieve a high dielectric constant as well as preserve the mechanical flexibility of the polymer.[9,10] The graphene is selected as the conductive filler because of its good electrical and thermal conductivity, high mechanical strength,

---

\*Corresponding author. Email: [xushuangxuan@163.com](mailto:xushuangxuan@163.com)

more importantly, large aspect ratio, and unique layered structure with nanoscale thickness.[11,12] The properties of graphene give advantages in the formation of a large number of parallel-board microcapacitors with low filler loading.[13] In literature, functionalization of graphene nanosheets surface by either oxidation procedure or physical adsorption/grafting protocols, such as thermally expanded graphene,[14] graphene oxide,[15] poly(vinyl alcohol) PVA-modified graphene,[12] and polymethyl methacrylate (PMMA)-modified graphene [16,17] have been used to make a positive impact on the dielectric properties of PVDF composites. He et al. [18] fabricated graphene/polymer composites by solvothermal reduction of graphene oxide in the polymer solution. It was found that only 0.5 vol.% solvothermal reduced graphene doping will increase the dielectric constant of the material from 7 to about 105. Fan et al. [3] prepared graphene/PVDF composites with a multilayered structure. A high dielectric constant of more than 340 at 100 Hz was obtained when the graphene volume fraction was 0.00177. Yang et al. [19] have reported that the PVDF-based composites with nickel particles coated multiwalled carbon nanotubes were prepared by solution blending and hot-press processing. And, the dielectric permittivity was as high as 290 at  $10^3$  Hz when the weight fraction of Ni-MWNTs was 10%.

In this work, we investigate the crystalline form of  $\beta$ -phase and dielectric properties of PVDF/exfoliated graphene (EG) composites with a variety of functionalized EG prepared by solution cast method. With the incorporation of different functionalized EG, the  $\beta$ -phase PVDF was achieved directly through a solution-casted route, which provides a facile way to fabricate piezoelectric PVDF composites. Besides, the effect of functionalized EG with different chemical groups on the formation of the  $\beta$ -phase in PVDF was systemically investigated, which can serve as a basis for the optimization of choosing appropriate EG for fabricating piezoelectric PVDF composites. Moreover, the factors determining the amount of  $\beta$ -phase and the reasons for dielectric properties evolution in PVDF composites filled with differently functionalized EG were analyzed by studying the surface functionalization of EG.

## 2. Experimental

### 2.1. Materials

Natural graphite powder was provided by Nanjing Xianfeng Nanomaterial Science and Technology Co., Ltd, China. PVDF (FR904) was purchased from Shanghai 3F New Materials Co., Ltd, China. N,N-dimethylacetamide (DMAc, >99.5%, reagent) was purchased from Tianjin Weichen Chemical Reagent Co., Ltd, China. Other reagents were purchased from Tianjin Reagents Co., Ltd and used without further purification.

### 2.2. Preparation of EG

EG was prepared by a two-step synthesis. Firstly, graphite oxide was prepared by the modified Hummers method [20] and then EG was obtained by thermal exfoliation from graphite oxide. In detail, a 9:1 mixture of concentrated  $\text{H}_2\text{SO}_4$  and  $\text{H}_3\text{PO}_4$  was added to a mixture of natural graphite flakes and  $\text{KMnO}_4$ , and the reaction was heated to  $50^\circ\text{C}$  and stirred for 12 h. The reaction was cooled to room temperature and poured onto ice (400 mL) with  $\text{H}_2\text{O}_2$  (30%, 3 mL). Then, the mixture was washed with deionized water until the pH value was up to 6 and then vacuum-dried at  $60^\circ\text{C}$  for 48 h. Finally, the prepared graphite oxide was thermally exfoliated in a vacuum tube furnace at the temperature of  $1050^\circ\text{C}$  for 30s,[21] yielding the EG.

### 2.3. Surface functionalization of EG

#### 2.3.1. Fluorination of EG

To form fluorinated graphene, the microwave plasma etcher (YZ-Z) was carried out to bring the process of the fluorination at room temperature with the  $\text{CF}_4$  flow. The chamber was evacuated to 5 Pa at room temperature. Then, the  $\text{CF}_4$  gas was inlet into the chamber, and the gas flow and pressure were controlled. The degree of fluorination process was adjusted by controlling the exposure time when the plasma treatment was carried out. The  $\text{CF}_4$  plasma treatment conditions for EG were as follows: gas flow rate of 1.5 L/h, operating pressure of 20 Pa, a bias of 200 V, the plasma power from 200 to 300 W, and process duration of 15 min.[22] The product was named as F-EG.

#### 2.3.2. Ozone modification of EG

The ozone modification of EG was performed under a continuous flow of ozone through EG beforehand placed into a three-neck flask. Ozone was produced in an ozone generator supplied by oxygen and then passed through the EG at a constant flow rate of 2 L/min. Ozone treatment temperature was 80 °C, and the treatment time was set for 20 min.[23] The generated graphene was named as  $\text{O}_3$ -EG.

#### 2.3.3. $\gamma$ -ray radiation induced functionalization of EG

The prepared EG was dispersed in acetone thoroughly by sonication, and a 10 mg/mL EG dispersion was obtained. Then methyl methacrylate (MMA) was added into the mixture. The resultant mixture was deoxygenated by bubbling high-purity nitrogen for 15 min and was then irradiated by  $\gamma$ -ray from a  $^{60}\text{Co}$  source in an absorbed dose 100 kGy with 0.8 kGy/h dose rate at room temperature. After irradiation, the EG-MMA mixture was purified repeatedly by cycling membrane filtration/acetone-redispersion until no white emulsion precipitated when the filtrate was added to water. The precipitate was then dried in a vacuum oven at 50 °C for 24 h to get EG grafted with polymethyl methacrylate (PMMA-g-EG).

### 2.4. Preparation of PVDF composites

The composites were prepared by solution cast method. At first, an amount of EG (0.5 wt.%) was dispersed in DMAc by ultrasonic treatment for 30 min. At the same time, PVDF was dissolved in DMAc by magnetic stirring. The suspension of graphene was then added into the PVDF/DMAc solution. Subsequently, the mixture was sonicated for 2 h and mechanically stirred at room temperature for 3 h. The composites were poured into uncovered glass dishes. The composites were then heated at 60 °C for 12 h under a vacuum to evaporate the residual solution. The thickness of the composites was 200–300  $\mu\text{m}$ . For comparison, PVDF, PVDF/F-EG (0.5 wt.%), PVDF/ $\text{O}_3$ -EG (0.5 wt.%), and PVDF/PMMA-g-EG (0.5 wt.%) sheets were also prepared by the same method.

### 2.5. Characterization

Atomic force microscopic (AFM) (Digital Instrument CSPM5500) measurements with the typical contact mode were performed to observe the morphology of different

surface-functionalized EG. X-ray photoelectron spectroscopy (XPS) investigations were carried out with a PHI 5700 ESCA System with Al K $\alpha$  (1486.6 eV) radiation to characterize changes of the chemical components of different surface-functionalized EG, and the pressure in the XPS analyzing vacuum chamber was less than  $3 \times 10^{-9}$  mbar. X-ray diffraction (XRD) characterizations of all samples were carried out in a Bruker D8 Discover using the CuK $\alpha$  radiation (0.154 nm) at a filament voltage of 40 kV and current of 100 mA. Fourier transform infrared spectroscopy (FTIR) was acquired using a Bruker Tensor 27 system in the 4000–800  $\text{cm}^{-1}$  wave-number range to observe crystallization of the PVDF and EG/PVDF composites. All the samples were pressed into a pellet with potassium bromide (KBr) before measurement. The spectra were collected by cumulating 32 scans at a resolution of 2  $\text{cm}^{-1}$ . The dielectric permittivity and dielectric loss of the composites were measured by means of broadband dielectric spectroscopy (BDS) in the frequency range of  $10^2$ – $10^7$  Hz, using an Alpha-N Frequency Response Analyser, supplied by Novocontrol. A BDS-1200, parallel-plate capacitor with two gold-plated electrodes system, supplied also by Novocontrol, was used as dielectric test cell.

### 3. Results and discussion

#### 3.1. Morphology and chemical characterizations of nanofillers

##### 3.1.1. AFM observations of EG

AFM measurements were used to characterize the surface topography changes of EG samples before and after modification.[24–26] As can be seen in Figure 1, there is an obvious difference among the EG, F-EG, O<sub>3</sub>-EG, and PMMA-EG. The thickness of the original EG is about 1.18 nm. However, after fluorination treatment, the thickness of the fluorinated EG samples is raised to 3.17 nm, which indicates that the F-EG samples are covered by the fluorine groups. Then, the thickness of the ozone modified EG samples is raised to 2.95 nm, which shows that the O<sub>3</sub>-EG samples are covered by the oxygen-containing groups. Compared with the other three samples, PMMA-g-EG has the thickness of 3.15 nm. The increase of thickness can be attributed to the PMMA chains on EG surface. As expected, by the modification processes (fluorination, ozonization, and modification with PMMA), the respective functional groups enrich on the EG surface and the EG sheets become thicker.

##### 3.1.2. XPS analysis of surface-functionalized EG

The element contents of EG, F-EG, O<sub>3</sub>-EG, and PMMA-g-EG samples were listed in Table 1. The contents of O element are improved by every modified treatment process. For the detailed studies of functional groups, peaks of C1s were studied. We used XPSPEAK41 software to fit the peaks and analyze the C1s spectra. And then, we calculate the chemical composition of all the functionalized EG samples by calculating the relative ratios of every chemical group's peak area Figure 2 and Table 2 show C1s peaks of XPS spectra of the functionalized EG samples before and after modification. The C1s spectra of EG, O<sub>3</sub>-EG, and PMMA-g-EG samples were deconvoluted into five peaks corresponding to C–C/C=C in aromatic rings (284.5 eV), C–OH bond (285 eV), epoxide group (286.2 eV), carbonyl group (287.4 eV), and additional carboxylate group (288.7 eV).[23] However, in the C1s spectrum of F-EG, a new band appears at approximately 290.3 eV which can be attributed to the C–F covalent bonds.[27,28]

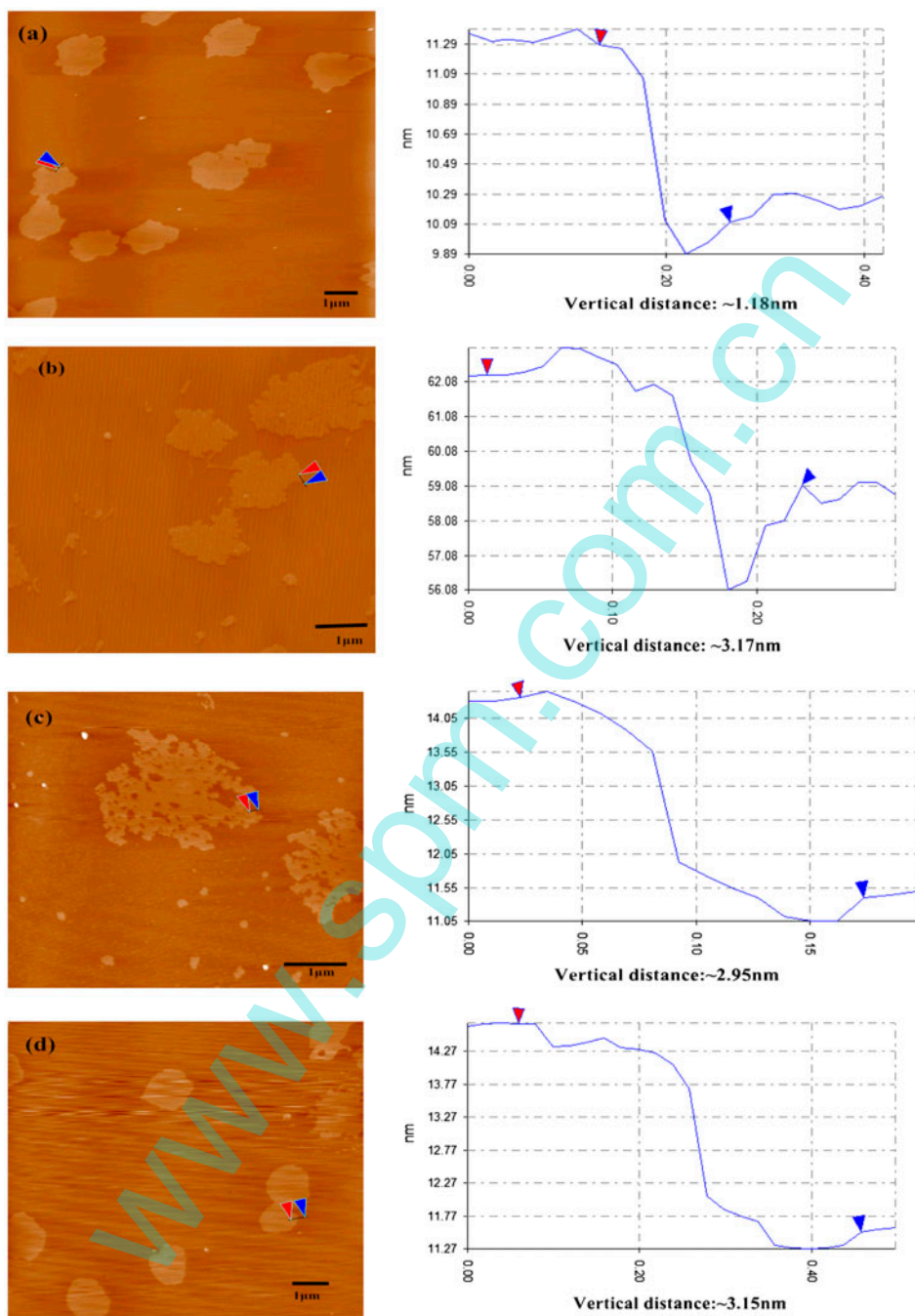
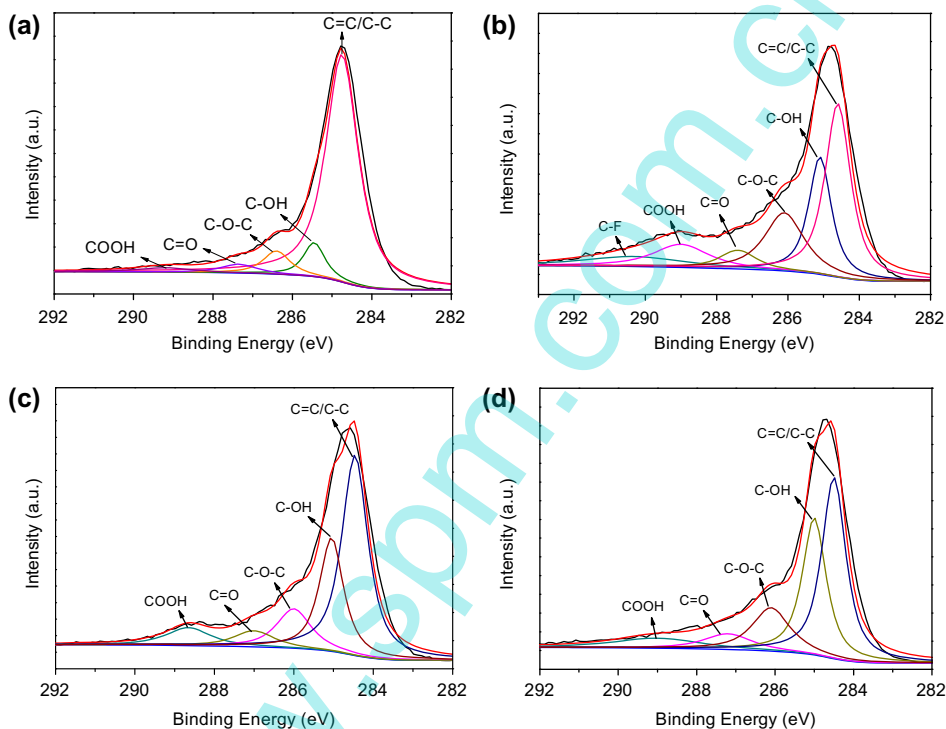


Figure 1. AFM images of (a) EG, (b) F-EG, (c) O<sub>3</sub>-EG, and (d) PMMA-g-EG.

Due to the modified treatment process, the percentage of C=C/C-C was lower whereas the percentage of oxygen-containing groups was higher than the untreated EG. Comparing the C1s spectra for all EG samples, it can be easily observed that all

Table 1. Element content of EG, F-EG, O<sub>3</sub>-EG and PMMA-g-EG samples.

| Sample             | C (%) | O (%) | F (%) |
|--------------------|-------|-------|-------|
| EG                 | 94.66 | 5.34  | –     |
| F-EG               | 66.04 | 20.35 | 13.61 |
| O <sub>3</sub> -EG | 78.71 | 21.29 | –     |
| PMMA-g-EG          | 84.58 | 15.42 | –     |

Figure 2. High resolution of C1s spectra of (a) EG, (b) F-EG, (c) O<sub>3</sub>-EG, and (d) PMMA-g-EG samples.Table 2. Chemical composition of EG, F-EG, O<sub>3</sub>-EG, and PMMA-g-EG samples.

| Sample             | Functional group (%) |       |       |       |      |      |
|--------------------|----------------------|-------|-------|-------|------|------|
|                    | C–C/C=C              | C–OH  | C–O–C | C=O   | COOH | C–F  |
| EG                 | 83.82                | 6.75  | 5.64  | 2.36  | 1.43 | –    |
| F-EG               | 37.68                | 21.60 | 18.50 | 5.60  | 8.67 | 7.95 |
| O <sub>3</sub> -EG | 48.78                | 22.46 | 13.46 | 6.68  | 8.62 | –    |
| PMMA-g-EG          | 38.51                | 15.72 | 28.71 | 11.83 | 6.23 | –    |



treatment at room temperature increased the C–OH, C=O, and COOH species with a simultaneous reduction of C=C/C–C. Meanwhile, the most worthy of our attention was that the percentage of C=O groups was more than 4 times increased compared with original EG in Table 2. The percentage of the C=O of the PMMA-g-EG sample was higher than that of the other three samples. In consequence, the content of C=O groups can be summarized as: PMMA-g-EG > O<sub>3</sub>-EG > F-EG > EG.

### 3.2. FTIR spectra of composites

In this work, FTIR spectra were used to further investigate the crystal structure of the PVDF composite films with different EG (as shown in Figure 3). The characteristic absorption peaks of the  $\alpha$ -phase appear at 766 and 1167 cm<sup>-1</sup>, and those of the  $\beta$ -phase appear at 837 and 1228 cm<sup>-1</sup>. [29]

In order to describe the variation of  $\beta$ -phase quantitatively, the relative percentage of  $\beta$ -phase ( $F_{(\beta)}$ ) in the whole crystalline phase is calculated according the following equation [30,31]:

$$F_{(\beta)} = \frac{X_{\beta}}{X_{\alpha} + X_{\beta}} = \frac{A_{\beta}}{1.26A_{\alpha} + A_{\beta}} \times 100\% \quad (1)$$

in which  $X_{\alpha}$  and  $X_{\beta}$  are crystalline mass fractions of  $\alpha$ -phase and  $\beta$ -phase, and  $A_{\alpha}$  and  $A_{\beta}$  are the absorbance of vibration bands at 766 and 837 cm<sup>-1</sup>, respectively. At least three positions on the composites were investigated by FTIR so that the standard deviation can be obtained.

The calculated relative percentage of  $\beta$ -phase ( $F_{(\beta)}$ ) is shown in Figure 4(a). Meanwhile, comparing the five composites, an obvious variation of the percentage of  $\beta$ -phase can be seen in Figure 4(a). And, it also indicates that PMMA-g-EG shows the highest contribution to the formation of  $\beta$ -phase, followed by O<sub>3</sub>-EG and F-EG, while sample containing EG has the lowest amount of  $\beta$ -phase. The formation of  $\beta$ -polymorph in EG-filled PVDF composites is attributed to the strong and specific interaction between the carbonyl group (C=O) found in graphene and the –CF<sub>2</sub> segments of the PVDF

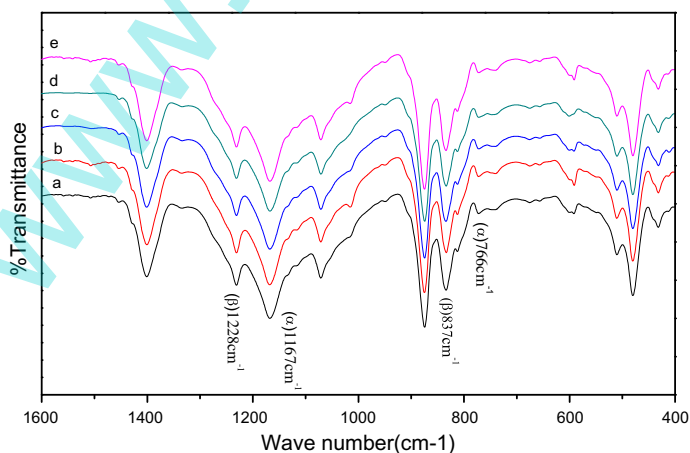


Figure 3. FTIR spectra of (a) PVDF, (b) EG/PVDF, (c) F-EG/PVDF, (d) O<sub>3</sub>-EG/PVDF, and (e) PMMA-g-EG/PVDF.

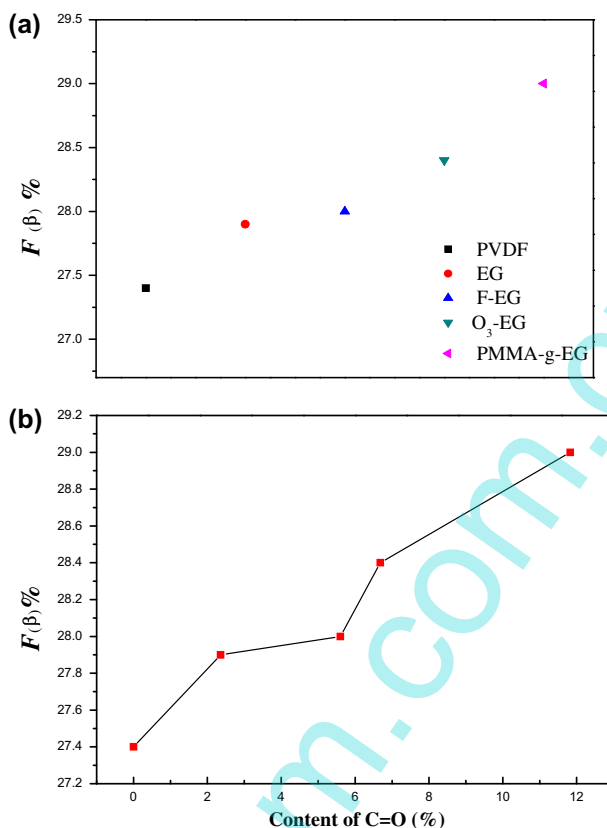


Figure 4. (a) Relative percentage of  $\beta$ -phase  $F_{(\beta)}$  in PVDF composites filled with different EG and (b) relative percentage of  $\beta$ -phase  $F_{(\beta)}$  in composites vs. the content of C=O.

polymer.[32] The enhancements of PMMA-g-EG composites could be explained by the specific interaction between the C=O group of PMMA and the  $CF_2$  group of PVDF.[33–35] This was previously explained by Layek et al. who used PMMA-modified graphene nanosheets as nucleating agents for  $\beta$ -phase in PVDF polymer composites.[16] Figure 4(b) shows that the relative percentage of  $\beta$ -phase  $F_{(\beta)}$  in composites vs. the C=O content for the selected composites. As shown in Figure 4(b), the beta-phase of PVDF increased from 27 up to 29% by addition of 0.5 wt.% modified EG. And the improvement in  $F_{(\beta)}$  is significantly improved as the content of C=O group increases.

### 3.3. XRD of composites

XRD measurements were carried out at  $2\theta$  angles from  $10^\circ$  to  $50^\circ$  to examine the crystalline phases in the solution-casted composite films (Figure 5). The peaks at  $18.4^\circ$  and  $38.5^\circ$  are assigned to the  $\alpha$ -phase and that at  $20.6^\circ$  belongs to the  $\beta$ -phase.[15,32] At the same time, the pattern at  $2\theta = 38.5^\circ$ , assigned to (0 0 2) lattice plane of  $\alpha$ -phase, is weaker in PMMA-g-EG/PVDF, followed by  $O_3$ -EG/PVDF, F-EG/PVDF and EG/PVDF. The reason for order is the different function of C=O and COOH, according to the



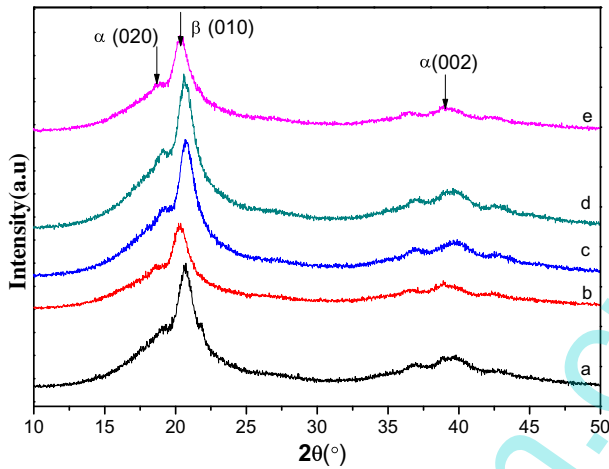


Figure 5. XRD of (a) PVDF, (b) EG/PVDF, (c) F-EG/PVDF, (d) O<sub>3</sub>-EG/PVDF, and (e) PMMA-g-EG/PVDF.

variation of the contents of C=O and COOH on the surface of functional graphene. Therefore, the results of XRD have the similar tendency of  $\beta$ -phase in composites with differently functionalized EG as evidenced by the results of FTIR.

### 3.4. Dielectric properties of the composites

Figure 6 shows the dielectric permittivity ( $\epsilon'$ ) of the composites with different functional EG nanosheets as a function of frequency at room temperature. The dielectric permittivity  $\epsilon'$ , which is also known as the relative dielectric constant, is the real part of the complex dielectric permittivity.[13,36,37] As shown in Figure 6, the dielectric

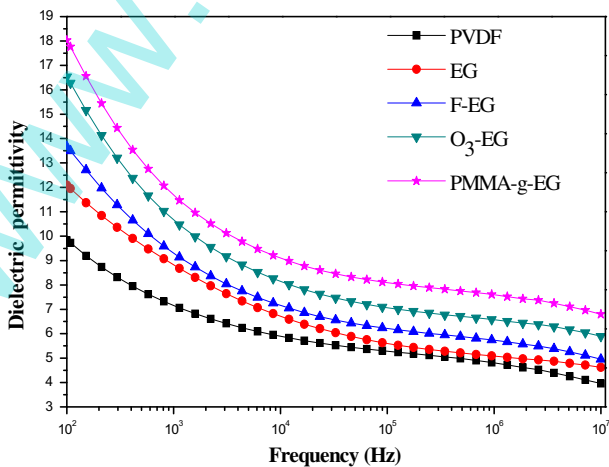


Figure 6. Dielectric permittivity of the PVDF, EG/PVDF, F-EG/PVDF, O<sub>3</sub>-EG/PVDF, and PMMA-g-EG/PVDF composites as function of frequency at room temperature.

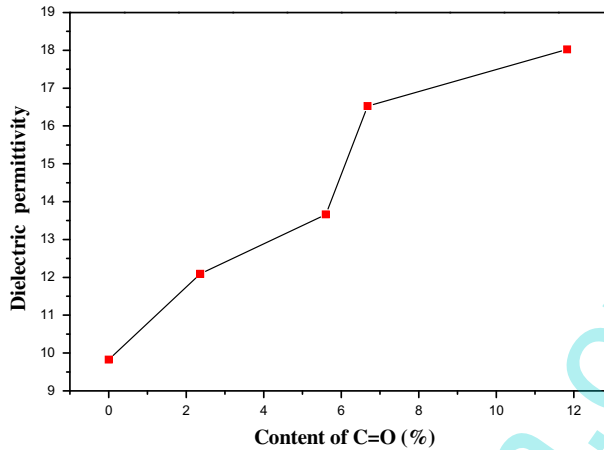


Figure 7. Dielectric permittivity at 100 Hz vs. the content of C=O.

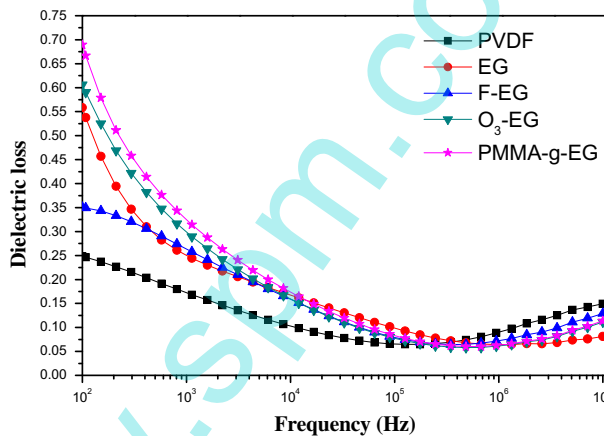


Figure 8. Dielectric loss of the PVDF, EG/PVDF, F-EG/PVDF, O<sub>3</sub>-EG/PVDF, and PMMA-g-EG/PVDF composites as function of frequency at room temperature.

constant measured at lower frequency is always greater than that at higher frequency. This frequency-dependent behavior is related to interfacial polarization, that is, Maxwell–Wagner–Sillars polarization.[18,36] In the frequency of  $10^2$ – $10^7$  Hz, the dielectric permittivity of pure PVDF gradually decreases from 9.8 to 4.0 as the increase of frequency. It can be clearly observed that the dielectric permittivity of the composites can be enhanced by blending with different functional EG nanosheets. Besides, the dielectric permittivity of the PMMA-g-EG/PVDF composites obtains 18 at 100 Hz, which is slightly lower than that reported in literature because of the different type of materials and test method.[18] The properties of enhancements are directly related to its specific interaction between the C=O group of PMMA and the CF<sub>2</sub> group of PVDF.[5,38] In consequence, the dielectric permittivity of conductive filler/PVDF composites can be summarized as: PMMA-g-EG > O<sub>3</sub>-EG > F-EG > EG. This order is attributed to the

aforementioned order of the content of C=O groups. Figure 7 displays the variation of the dielectric permittivity with the C=O content for EG/PVDF composites at 100 Hz. And, there is a linear relationship between the dielectric permittivity and the C=O content.

Figure 8 shows the dielectric loss ( $\tan \delta = \epsilon''/\epsilon'$ ) of the composites as a function of frequency at room temperature. The dielectric loss is commonly used as a measure of the energy dissipation in a dielectric material. It can be observed from Figure 6 that the dielectric loss of five kinds of composite films trends to reduce firstly and then increase with frequency from  $10^5$  to  $10^7$  Hz. This is an obvious relaxation loss process related to the PVDF polymer. And, the value of dielectric loss of the F-EG composite film is lower than that of the other binary composite films at 100 Hz. It may be because of the fact that the superior interfaces in the F-EG/PVDF composite are formed due to the better specific interaction between fluorine group ( $\text{CF}_2$ ) in F-EG surface and PVDF.

#### 4. Conclusion

In conclusion, the modified methods of graphene nanosheets are presented in this article. The dielectric properties of PVDF were enhanced by adding functionalized EG at the concentration of 0.5 wt.%. The results of AFM and XPS demonstrated that some functional groups and PMMA chains have been successfully grafted onto graphene nanosheets. PVDF-based composites filled with functionalized EG were successfully fabricated by solution cast method. The composites were carefully characterized by FTIR and XRD. Effects of functionalized EG on the formation of  $\beta$ -phase PVDF were investigated. As a result, carbonyl groups contribute to the formation of the  $\beta$ -phase. The composites showed high dielectric permittivity as compared with the control blends with high loss tangent. It is found that PMMA-g-EG doping will increase the dielectric constant of PVDF from 9.5 to 18. Such a dielectric performance is superior to that of other functionalized EG reinforced composites. The contents of  $\beta$ -phase and dielectric permittivity increased along with the increase of the C=O content.

#### Funding

The work was funded by the National Natural Science Foundation of China [grant number 11175130] and the Petrochemical Joint Funds of National Natural Science Fund Committee – China National Petroleum Corporation [grant number U1362108].

#### References

- [1] Yang C, Lin Y, Nan CW. Modified carbon nanotube composites with high dielectric constant, low dielectric loss and large energy density. *Carbon*. 2009;47:1096–1101.
- [2] Yu SS, Zheng WT, Yu WX, Zhang YJ, Jiang Q, Zhao ZD. Formation mechanism of beta-phase in PVDF/CNT composite prepared by the sonication method. *Macromolecules*. 2009;42:8870–8874.
- [3] Fan P, Wang L, Yang JT, Chen F, Zhong MQ. Graphene/poly(vinylidene fluoride) composites with high dielectric constant and low percolation threshold. *Nanotechnology*. 2012;23:8.
- [4] Eswaraiiah V, Balasubramaniam K, Ramaprabhu S. Functionalized graphene reinforced thermoplastic nanocomposites as strain sensors in structural health monitoring. *J. Mater. Chem*. 2011;21:12626–12628.
- [5] Mandal A, Nandi AK. Noncovalent functionalization of multiwalled carbon nanotube by a polythiophene-based compatibilizer: reinforcement and conductivity improvement in poly(vinylidene fluoride) films. *J. Phys. Chem. C*. 2012;116:9360–9371.

- [6] Dang ZM, Yuan JK, Yao SH, Liao RJ. Flexible nanodielectric materials with high permittivity for power energy storage. *Adv. Mater.* 2013;25:6334–6365.
- [7] Ansari S, Giannelis EP. Functionalized graphene sheet-poly(vinylidene fluoride) conductive nanocomposites. *J. Polym. Sci. Part B-Polym. Phys.* 2009;47:888–897.
- [8] Zhang JG, Xu ZW, Mai W, Min CY, Zhou BM, Shan MJ, Li YL, Yang CY, Wang Z, Qian XM. Improved hydrophilicity, permeability, antifouling and mechanical performance of PVDF composite ultrafiltration membranes tailored by oxidized low-dimensional carbon nanomaterials. *J. Mater. Chem. A.* 2013;1:3101–3111.
- [9] Tjong SC. Polymer composites with graphene nanofillers: electrical properties and applications. *J. Nanosci. Nanotechnol.* 2014;14:1154–1168.
- [10] Dang ZM, Yuan JK, Zha JW, Zhou T, Li ST, Hu GH. Fundamentals, processes and applications of high-permittivity polymer matrix composites. *Prog. Mater. Sci.* 2012;57:660–723.
- [11] Georgakilas V, Otyepka M, Bourlinos AB, Chandra V, Kim N, Kemp KC, Hobza P, Zboril R, Kim KS. Functionalization of graphene: covalent and non-covalent approaches derivatives and applications. *Chem. Rev.* 2012;112:6156–6214.
- [12] Tantis I, Psarras GC, Tasis D. Functionalized graphene – poly(vinyl alcohol) nanocomposites: physical and dielectric properties. *Express Polym. Lett.* 2012;6:283–292.
- [13] He F, Lau S, Chan HL, Fan JT. High dielectric permittivity and low percolation threshold in nanocomposites based on poly(vinylidene fluoride) and exfoliated graphite nanoplates. *Adv. Mater.* 2009;21:710–715.
- [14] Ramanathan T, Abdala AA, Abdala AA, Stankovich S, Dikin DA, Herrera-Alonso M, Piner RD, Adamson DH, Schniepp HC, Chen X, Ruoff RS, Nguyen ST, Aksay IA, Prud'homme RK, Brinson LC. Functionalized graphene sheets for polymer nanocomposites. *Nat. Nanotechnol.* 2008;3:327–331.
- [15] Rahman MA, Chung GS. Synthesis of PVDF-graphene nanocomposites and their properties. *J. Alloys Compd.* 2013;581:724–730.
- [16] Layek RK, Samanta S, Chatterjee DP, Nandi AK. Physical and mechanical properties of poly(methyl methacrylate)-functionalized graphene/poly(vinylidene fluoride) nanocomposites piezoelectric beta polymorph formation. *Polymer.* 2010;51:5846–5856.
- [17] Wang DR, Bao YR, Zha JW, Zhao J, Dang ZM, Hu GH. Improved dielectric properties of nanocomposites based on poly(vinylidene fluoride) and poly(vinyl alcohol)-functionalized graphene. *ACS Appl. Mater. Interfaces.* 2012;4:6273–6279.
- [18] He LX, Tjong SC. Low percolation threshold of graphene/polymer composites prepared by solvothermal reduction of graphene oxide in the polymer solution. *Nanoscale Res. Lett.* 2013;8:7.
- [19] Yang DD, Xu HP, Wang JR, Wu YH. Nickel-multiwalled carbon nanotubes/polyvinylidene fluoride composites with high dielectric permittivity. *J. Appl. Polym. Sci.* 2013;130:3746–3752.
- [20] Marcano DC, Kosynkin DV, Berlin JM, Sinitskii A, Sun ZZ, Slesarev A, Alemany LB, Lu W, Tour JM. Improved synthesis of graphene oxide. *ACS Nano.* 2010;4:4806–4814.
- [21] Shi CB, Chen L, Xu ZW, Jiao YA, Li YL, Wang CH, Shan MJ, Wang Z, Guo QW. Monitoring influence of chemical preparation procedure on the structure of graphene nanosheets. *Physica E.* 2012;44:1420–1424.
- [22] Shen C, Huang GS, Cheng YC, Cao RG, Ding F, Schwingenschlogl U, Mei YF. Thinning and functionalization of few-layer graphene sheets by CF<sub>4</sub> plasma treatment. *Nanoscale Res. Lett.* 2012;7:8.
- [23] Xu ZW, Yue MY, Chen L, Zhou BM, Shan MJ, Niu JR, Li BD, Qian XM. A facile preparation of edge etching, porous and highly reactive graphene nanosheets via ozone treatment at a moderate temperature. *Chem. Eng. J.* 2014;240:187–194.
- [24] Chen J, Yao BW, Li C, Shi GQ. An improved Hummers method for eco-friendly synthesis of graphene oxide. *Carbon.* 2013;64:225–229.
- [25] Wang SJ, Geng Y, Zheng QB, Kim JK. Fabrication of highly conducting and transparent graphene films. *Carbon.* 2010;48:1815–1823.
- [26] Stankovich S, Dikin DA, Piner RD, Kohlhaas KA, Kleinhammes A, Jia Y, Wu Y, Nguyen ST, Ruoff RS. Synthesis of graphene-based nanosheets via chemical reduction of exfoliated graphite oxide. *Carbon.* 2007;45:1558–1565.

- [27] Bon SB, Valentini L, Verdejo R, Garcia Fierro JLG, Peponi L, Lopez-Manchado MA, Kenny JM. Plasma fluorination of chemically derived graphene sheets and subsequent modification with butylamine. *Chem. Mat.* 2009;21:3433–3438.
- [28] Wang ZF, Wang JQ, Li ZP, Gong PW, Liu XH, Zhang LB, Ren JF, Wang HG, Yang SR. Synthesis of fluorinated graphene with tunable degree of fluorination. *Carbon.* 2012;50:5403–5410.
- [29] Salimi A, Yousefi AA. FTIR studies of beta-phase crystal formation in stretched PVDF films. *Polym. Test.* 2003;22:699–704.
- [30] Cardoso VF, Minas G, Lanceros-Méndez S. Multi layer spin-coating deposition of poly(vinylidene fluoride) films for controlling thickness and piezoelectric response. *Sens Actuator A-Phys.* 2013;192:76–80.
- [31] Ke K, Pötschke P, Jehnichen D, Fischer D, Voit B. Achieving beta-phase poly(vinylidene fluoride) from melt cooling: effect of surface functionalized carbon nanotubes. *Polymer.* 2014;55:611–619.
- [32] El Achaby M, Arrakhiz FZ, Vaudreuil S, Essassi EM, Qaiss A. Piezoelectric beta-polymorph formation and properties enhancement in graphene oxide – PVDF nanocomposite films. *Appl. Surf. Sci.* 2012;258:7668–7677.
- [33] El Achaby M, Arrakhiz FE, Vaudreuil S, Essassi E, Qaiss A, Bousmina M. Nanocomposite films of poly(vinylidene fluoride) filled with polyvinylpyrrolidone-coated multiwalled carbon nanotubes: enhancement of ss-polymorph formation and tensile properties. *Polym. Eng. Sci.* 2013;53:34–43.
- [34] Sharma M, Madras G, Bose S. Size dependent structural relaxations and dielectric properties induced by surface functionalized MWNTs in poly(vinylidene fluoride)/poly(methyl methacrylate) blends. *Phys. Chem. Chem. Phys.* 2014;16:2693–2704.
- [35] Sharma M, Madras G, Bose S. Cooperativity and structural relaxations in PVDF/PMMA blends in the presence of MWNTs: an assessment through SAXS and dielectric spectroscopy. *Macromolecules.* 2014;47:1392–1402.
- [36] Shang JW, Zhang YH, Yu L, Shen B, Lv FZ, Chu PK. Fabrication and dielectric properties of oriented polyvinylidene fluoride nanocomposites incorporated with graphene nanosheets. *Mater. Chem. Phys.* 2012;134:867–874.
- [37] Shang JW, Zhang YH, Yu L, Luan XL, Shen B, Zhang ZL, Lv FZ, Chu PK. Fabrication and enhanced dielectric properties of graphene-polyvinylidene fluoride functional hybrid films with a polyaniline interlayer. *J. Mater. Chem. A.* 2012;1:884–890.
- [38] Mandal A, Nandi AK. Physical properties of poly(vinylidene fluoride) composites with polymer functionalized multiwalled carbon nanotubes using nitrene chemistry. *J. Mater. Chem.* 2011;21:15752–15763.